ACS OMEGA

Open Access

http://pubs.acs.org/journal/acsodf

Article

Supramolecular Chemotherapy: Complexation by Carboxylated Pillar[6]arene for Decreasing Cytotoxicity of Nitrogen Mustard to Normal Cells and Enhancing Its Antitumor Efficiency against Breast Cancer

Jin Long Zhang,* Xiao Wei Zhang, Bing Yuan, Heng Zhang, Xing Zhi Wang, Hao Wang, and Hong Wei Zhao

Cite This: *ACS Omega* 2024, 9, 11829−11835

Read Online

ACCESS | Metrics & More | Article Recommendations | Supporting Information

ABSTRACT: Advances in chemotherapeutic strategies are urgently required to improve antitumor efficiency. Herein, a carboxylated pillar[6]arene (CP6A) was employed to load chemotherapy medication, nitrogen mustard (NM), via forming a direct host−guest complex, as this helps to decrease the cytotoxicity of NM on normal mammary epithelial cells. Attributed to the stronger complexation ability of CP6A for endogenous spermine (SPM) than for NM, the complexed NM could be competitively released from the CP6A cavity via replacement with SPM. This chemotherapy strategy performed well in vitro and in vivo for SPM-overexpressed cancers. In comparison with free NM, antitumor efficiency of NM/CP6A was significantly enhanced, which originated from the synergistic effect of competitive release of NM and simultaneous trapping of SPM. This strategy might guide expansion to other first-line antitumor agents to improve therapeutic efficacy and decrease side effects, thereby replenishing the possibilities of supramolecular chemotherapy.

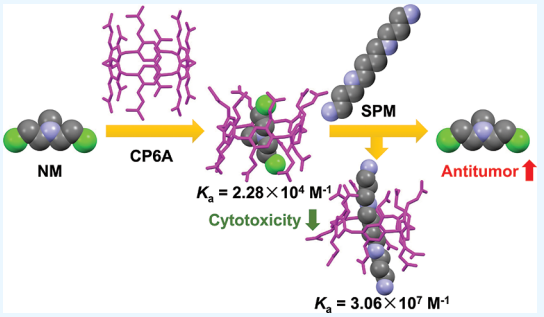

INTRODUCTION

Cancer is chiefly responsible for global mortality, and patient numbers are estimated at more than 21 million by 2030.[1] Of all types of carcinomas, breast cancer is one of the most common malignancies and is reported to have an increasing trend of incidence and mortality, seriously affecting a large number of female patients.[2] The age of patients with breast cancer is also tending toward younger females, and it is hard to implement recovery due to its high ratio of recurrence.[3,4] Owing to this, advanced therapeutic regimens are urgently required to boost treatment outcomes. Although a tremendous amount of effort has been devoted to improving curative strategies for breast cancer, chemotherapy is still perceived as the leading clinical treatment.[5] Nonetheless, a lot of antitumor drugs have substantial flaws, such as ambiguous efficacy, high cytotoxicity, and tumor resistance, which restricts them from successful therapeutic applications.[6,7] In recent years, massive efforts have been made to develop multitudinous delivery systems, including micelles,[8,9] liposomes,[10,11] vesicles,[12,13] and other nanocarriers[14,15] to increase therapeutic efficacy and reduce side effects of chemotherapeutic agents.

Supramolecular chemotherapy was born from the amalgamation between supramolecular chemistry and chemotherapy, and it offers an available and generally applicable approach by which to enhance therapeutic efficacy of chemotherapy medicationin tumor cells and decrease side effects in normal cells.[16−19] The core of this approach is one certain biomarker, overexpression, which exists in the tumor microenvironment. Biomarker-triggered replacement of chemotherapy medication and synchronous trapping of biomarkers by intermolecular forces can exert synergistic improvements in treatment outcomes.[20−22] Spermine (SPM) is naturally present in majority of living entities and regulates many physiological activities, such as cellular differentiation and multiplication.[23] Maintaining a balance of SPM through integrated function between synthesis, metabolism, and transshipment is critical to cell survival.[24] Tumor cells, which rapidly divide, need large amounts of SPM to support cell division.[25] Previous research has shown that depleting SPM via host−guest complexation by artificial receptors could induce the apoptosis of tumor cells.[20−22] In light of this, SPM has promise as a biomarker in the current study.

Received: November 27, 2023
Revised: February 8, 2024
Accepted: February 14, 2024
Published: February 29, 2024

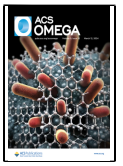

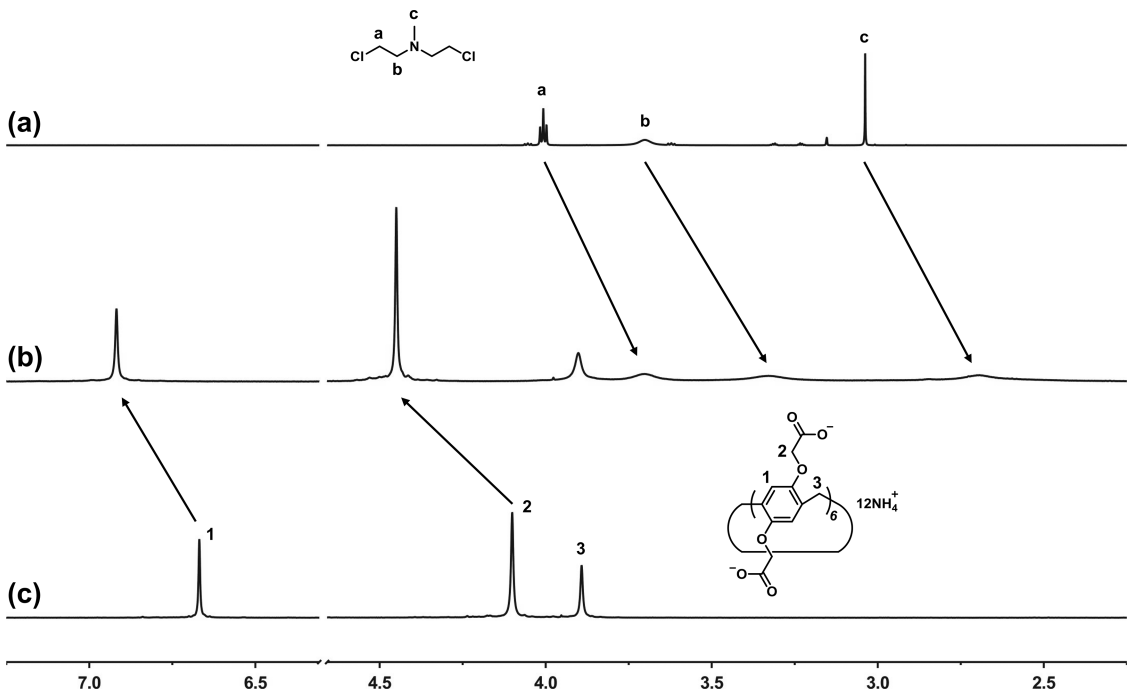

Figure 1. Partial ^{1}H NMR spectra (600 MHz) of (a) NM (5.0 mM), (b) NM (5.0 mM) with CP6A (5.0 mM), and (c) CP6A (5.0 mM) in deuterated PBS at pH 7.4.

As evidence of concept, nitrogen mustard (NM), the first effective chemotherapy drug against many forms of cancer,[26,27] was chosen as a guest drug. A widely used macrocycle, carboxylated pillar[6]arene (CP6A), served as a macrocyclic receptor because of its excellent water-solubility and appropriate size/charge with both NM and SPM (Figure 1).[16,28−32] Robust complexation ability to NM is essential to ensure that systemic side effects are avoided. In addition, stronger binding to SPM is a prerequisite for competitive replacement of bound NM. SPM trapped by CP6A was expected to synergistically improve the antitumor efficacy. In addition, overexpression of SPM in the tumor microenvironment helped to trigger release of NM from the macrocyclic cavity. Consequently, supramolecular chemotherapy embodied in NM/CP6A can be employed to enhance chemotherapeutic efficacy of NM and relieve the associated severe systemic toxicity (Scheme 1).

RESULTS AND DISCUSSION

In this investigation, the complexation behavior between host (CP6A) and guests (NM and SPM) was first investigated by ^{1}H NMR spectroscopy. Figure 1 shows the spectra of NM with and without CP6A in deuterated phosphate-buffered saline (PBS) at pH 7.4. In the presence of an equivalent amount of host, the proton signals for H_a, H_b, and H_c of NM were found to exhibit remarkable upfield shifts and broadening effects in comparison with free NM ($\Delta\delta$ = −0.31 to −0.37 ppm). This indicated that these protons were encapsulated by CP6A and shielded from the electron-rich macrocyclic cavity by the formation of a host−guest complex. CP6A also showed complex behavior similar to that of SPM (Figure S1). The resonance peaks related to SPM, especially for H_d and H_e, substantially shifted upfield ($\Delta\delta$ = −0.48 ppm for H_d and −0.39 ppm for H_e) and coupled with broadening phenomenon, reaveling a host−guest complex of SPM/CP6A. In addition, geometry optimization of NM/CP6A and SPM/CP6A was performed by a MM2 minimized molecular model (Figure S2). The above results led us to suggest that NM was entirely encapsulated within the macrocyclic cavity, and the middle methylenes of SPM were immersed in the cavity of CP6A in its axial orientation.

Scheme 1. Chemical Structures of CP6A and NM

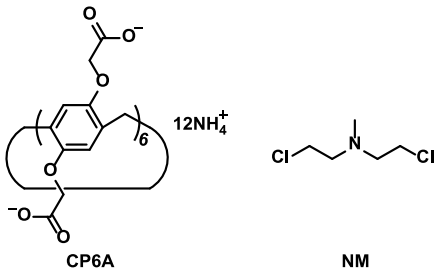

The association constants (K_a) of CP6A with NM and SPM were quantitatively measured by fluorescence titration tests. First, the continuous variation method (Job's plot) was utilized to prove that complexation behavior of the host−guest complex was consistent with a 1:1 binding stoichiometry (Figure 2a,b). Following a mixture with NM, fluorescence intensity of CP6A increased gradually, probably because the conformation of CP6A was fixed and intramolecular rotation was restricted upon guest binding. The K_a value of NM/CP6A was measured to be (2.28 ± 0.15) × 10^4 M^{-1} using standard curve fitting protocols (Figure 2c). Robust binding to NM was essential to ensuring that off-target leaking was avoided in the body. Compared to the K_a value of SPM/CP6A [(3.06 ± 0.48) × 10^7 M^{-1}, Figure 2d], stronger complexation ability would endow SPM with potency to competitively replace NM from the NM/CP6A complex. To further investigate whether NM could be efficiently released from the NM/CP6A complex by competitive replacement with SPM, ^{1}H NMR titration were

https://doi.org/10.1021/acsomega.3c09353
ACS Omega 2024, 9, 11829−11835

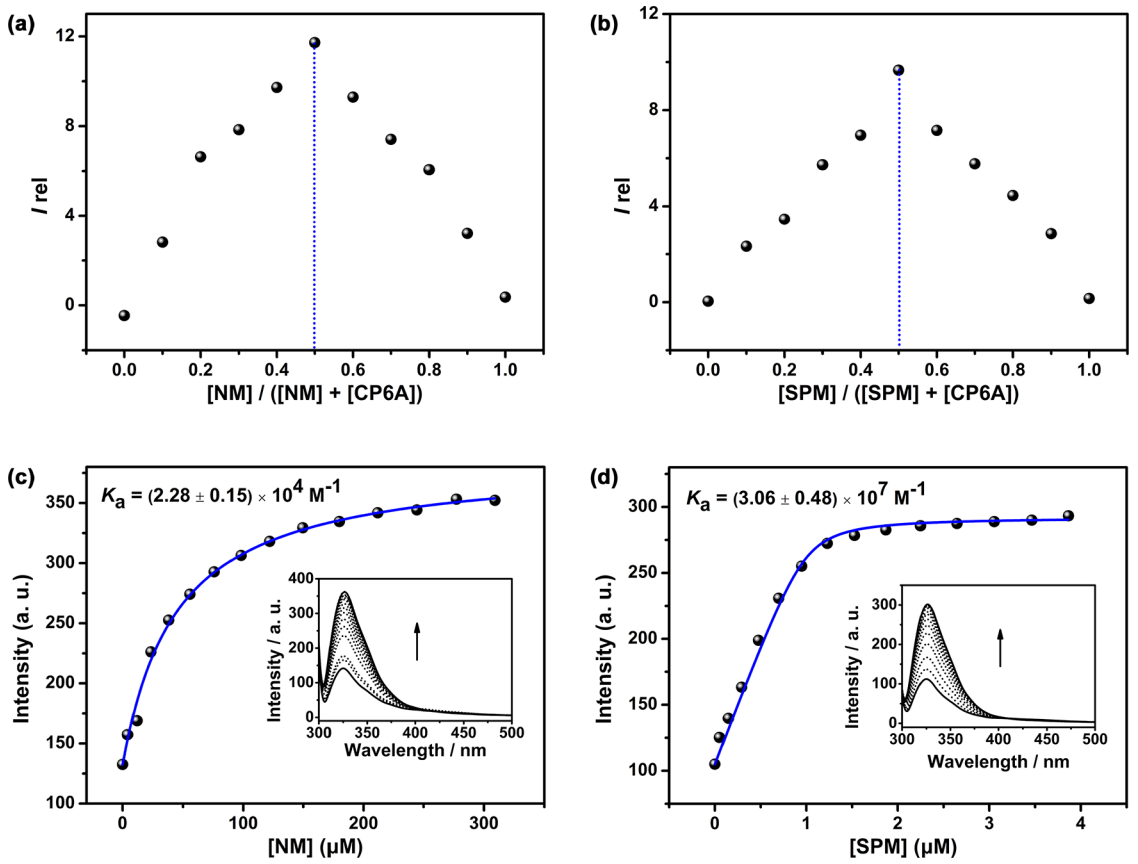

Figure 2. (a) Job's plot for CP6A with NM in 10 mM PBS at pH 7.4 (λ_{ex} = 290 nm, λ_{em} = 330 nm, [CP6A] + [NM] = 8.0 μM). (b) Job's plot for CP6A with SPM in 10 mM PBS at pH 7.4 (λ_{ex} = 290 nm, λ_{em} = 330 nm, [CP6A] + [SPM] = 2.0 μM). (c) Associated titration curve of CP6A (1.00 μM) with NM consistent with a 1:1 binding stoichiometry (λ_{em} = 330 nm, λ_{ex} = 290 nm for the fluorescent titration test). (d) Associated titration curve of CP6A (1.00 μM) with SPM consistent with a 1:1 binding stoichiometry (λ_{em} = 330 nm, λ_{ex} = 290 nm for the fluorescent titration test).

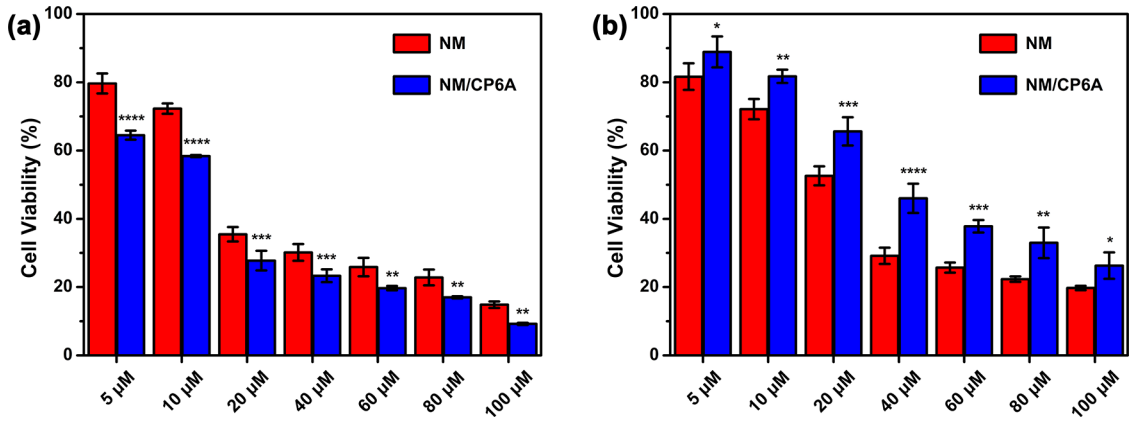

Figure 3. (a) In vitro antitumor activity of NM/CP6A and comparison with NM after incubation for 48 h in the MCF-7 cell line. (b) Cytotoxicity in MCF-10A cells incubated for 48 h. Data shown are the mean ± SD for n = 5. Significant differences were assessed using the two-way ANOVA with multiple comparisons. *P < 0.05, **P < 0.01, ***P < 0.001, and ****P < 0.0001.

conducted to characterize the process of competitive binding at physiological pH (7.4). A series of SPM varying from 0.5 to 2.0 equiv was quantitatively added into NM/CP6A (2.0/2.0 mM). As shown in Figure S3, with the increase of SPM, the proton peaks related to NM gradually shifted downfield and became clear. While the signals of the protons on SPM underwent upfield shift, suggesting that SPM occupied the host cavity of CP6A. These results revealed a complete release of NM from NM/CP6A because the binding affinity of SPM with CP6A was 3 orders of magnitude higher than that of NM with CP6A.

Prior to therapeutic efficacy studies, the toxicity of CP6A in human normal mammary epithelial (MCF-10A) and breast adenocarcinoma (MCF-7) cells was investigated via CCK-8 assays. CP6A showed remarkably low cytotoxicity during 48 h of incubation periods. For instance, cell viability was kept at 97.30(±1.92) and 96.81(±1.86)% after treatment with 100 μM CP6A for MCF-7 and MCF-10A cells (Figure S4). Furthermore, changes in weight and behavior of mice were

https://doi.org/10.1021/acsomega.3c09353
ACS Omega 2024, 9, 11829−11835

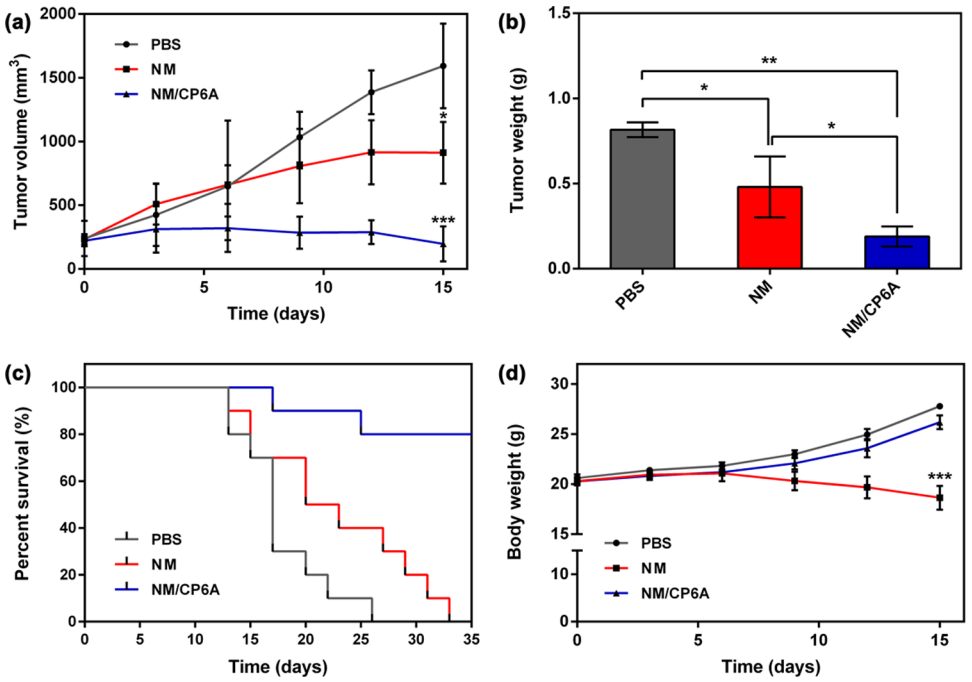

Figure 4. In vivo antitumor efficacy studies. (a) Tumor growth curves of the MCF-7 xenograft mice in the groups dealed with PBS, NM, and NM/CP6A (mean ± SD, $n = 3$). (b) Normalized tumor weight 15 days after treatment with PBS, NM, and NM/CP6A (mean ± SD, $n = 3$). (c) Survival rate of mice bearing MCF-7 tumors after different treatments ($n = 10$ mice per group). (d) Changes in body weight of MCF-7 xenograft nude mice after different treatments (mean ± SD, $n = 3$). Significant differences were assessed in (a), (b), and (d) using the one-way ANOVA with multiple comparisons. $^{*}P < 0.05$, $^{**}P < 0.01$, and $^{***}P < 0.001$.

monitored for 15 days after intravenous administration of 42 mg·kg^{-1} CP6A and related data were recorded at predetermined intervals to investigate the biocompatibility of CP6A (Figure S5). In comparison with mice administered PBS, a similar weight fluctuation curve was seen for mice treated with CP6A. In addition, after treatment with CP6A, mice exhibited slight differences in their physical, social, and dietary behaviors. These favorable findings indicated that CP6A could be safely applied to subsequent biological evaluations.

Next, the in vitro cellular inhibition efficiency of NM/CP6A was investigated in the same MCF-7 and MCF-10A cells, where cells incubated with free NM were used as controls. Concentration-dependent cell death was observed in all groups, as shown in Figure 3a,b. The half-maximum inhibition concentration (IC_{50}) of NM in the MCF-7 cell line was determined to be 18.08 μM (Table S1). In comparison, NM/CP6A presented stronger antitumor potency than free NM. The remarkable improvement in antitumor potency was ascribed to the replacement of NM from the CP6A cavity via confronting overexpression of SPM in the tumor microenvironment and trapping SPM to restrict its normal physiological effects by the formation of a stable host−guest SPM/CP6A complex. Moreover, via direct encapsulation, the toxicity of NM/CP6A in MCF-10A cells was found to be significantly reduced. This was because cytotoxicity is always concentration-dependent, and host−guest complexation can reduce the concentration of free toxic drugs. SPM levels in non-neoplastic cell lines are often less than those in tumor cell lines, and a low concentration of SPM was inadequate to thoroughly replace NM via competitive binding.

Furthermore, in vivo, the therapeutic efficiency of NM/CP6A was evaluated by a subcutaneous xenograft mouse model of breast adenocarcinoma. The tumor volume of mice administered PBS after 15 days increased by approximately 6.66 times from initial volume. Mice treated with both NM and the NM complex exhibited a certain amount of tumor growth inhibition (Figure 4a). In comparison with the PBS group, the NM group showed 42.75% inhibitory efficacy. Administration of NM/CP6A resulted in more efficient inhibition of tumor proliferation (87.61%). In addition, the normalized tumor weight was measured to assess the efficacy of NM/CP6A (Figure 4b). The tumor weight of mice treated with PBS (0.82 ± 0.04 g) was 70.83% greater than that of mice treated with NM (0.48 ± 0.18 g) and 331.58% greater than that of those treated with NM/CP6A (0.19 ± 0.06 g). The results of a Kaplan−Meier analysis revealed that the median survival of tumor-bearing mice administered NM/CP6A was significantly prolonged (over 35 days) when compared to those that received PBS and free NM (17 and 23 days, respectively; Figure 4c). In addition, pathological slice staining and immunohistochemical assay were carried out to assess the treatment outcomes of different formulations (Figure S6). Hematoxylin and eosin (H&E)-stained tumor tissue of mice administered PBS presented unbroken cellular structures, indicating a rapid growth state. In comparison with the PBS group, both free NM and NM/CP6A groups exhibited a degree of necrocytosis. Remarkably, cellular edemas and nuclear shrinkage were observed in the mice that were administered NM/CP6A. Moreover, the results of the terminal deoxynucleotidyl transferase dUTP nick end labeling (TUNEL) assay verified that administration of NM/CP6A resulted in more severe cell apoptosis. In clinical settings, NM can induce several toxicity-related side reactions. In this study, weight fluctuation of mice after treatment with various formulations was used as a representation of side effects. The body weights of mice administered free NM increased and

https://doi.org/10.1021/acsomega.3c09353
ACS Omega 2024, 9, 11829−11835

then decreased. For comparison, the mean body weight of the NM/CP6A group increased from 20.29 ± 0.40 to 26.20 ± 0.69 g, and weight trends were similar to mice that were administered PBS (Figure 4d). Taken together, these results supported the conclusion that the complexation of NM with CP6A could enhance the chemotherapeutic efficacy of NM and decrease its associated severe systemic toxicity in vivo.

MATERIALS AND METHODS

Materials. All reagents were purchased commercially and used without further purification unless otherwise noted. Carboxylated pillar[6]arene (CP6A) was synthesized and purified according to a previously reported procedure.[28] NM was purchased from Aladdin (Shanghai, China). Spermine (SPM) was purchased from Innochem (Beijing, China). Dulbecco's modified Eagle medium (DMEM) was purchased from Thermo Fisher Scientific. Fetal bovine serum (FBS), penicillin-streptomycin, and PBS were purchased from Gibco (Thermo Fisher Scientific). Cell counting kit-8 (CCK-8) was purchased from Dojindo Co., Ltd. (Shanghai, China). Human breast adenocarcinoma (MCF-7) and normal human mammary epithelial cells (MCF-10A) were obtained from the Cell Bank of the Chinese Academy of Sciences.

Instruments. ^{1}H NMR data were recorded on a Bruker Advance 600 MHz spectrometer. Fluorescence spectroscopic studies were carried out using a FL 6500 fluorescence spectrophotometer, PerkinElmer, Inc. Cytotoxicity studies were performed on SpectraMax M5 plate reader, Molecular Devices.

Cells and Animals. MCF-7 and MCF-10A cells were cultured in DMEM supplemented with 10% FBS, 1% penicillin, and 1% streptomycin. The cells were then incubated at 37 °C under 5% CO_2 and 90% relative humidity and passaged every 2 days.

Six-week-old female BALB/c nude mice were purchased from SPF Biotechnology Co. Ltd. (Beijing, China) and maintained at 25 °C in a 12 h light/dark cycle with free access to food and water. Mice were allowed to acclimate to the environment for at least 1 week before the experiments. Animal experiments were approved by the ethics and welfare review of laboratory animals at Beijing Tongren Hospital Affiliated to Capital Medical University (TRLAWEC2022-2096) and adhered to the ARRIVE guidelines.

NMR Spectroscopy. Samples for 1:1 ^{1}H NMR spectra were prepared in pH 7.4 deuterated phosphate buffer (10 mM). All NMR spectra were acquired at 298 K in the solution state.

Fluorescence Titration. To determine the association constant between the host (CP6A) and the two guests (NM and SPM), direct fluorescence titration of CP6A (1 μM) with various concentrations of NM and SPM was carried out in 10 mM PBS at pH 7.4, as previously reported.[33]

In Vitro Cytotoxicity. The relative cytotoxicity of the samples against two cell lines (MCF-7 and MCF-10A) was assessed using the CCK-8 assay according to the manufacturer's instructions. MCF-7 and MCF-10A cells were seeded into 96-well plates at a density of 8000 cells/well in 100 μL of DMEM supplemented with 10% FBS, 1% penicillin, and 1% streptomycin and then cultured for 24 h in 5% CO_2 at 37 °C. Several formulations were dissolved in PBS and diluted to the required concentration and then added to the cell-containing wells which were further incubated at 37 °C under 5% CO_2 for 48 h. Subsequently, 10 μL of CCK-8 was added into each well, and the mixture was incubated for another 1 h. Absorbance of the plates was measured at 450 nm by using a plate reader:

$$\text{Viability}(\%) = \frac{A - A_b}{A_0 - A_b}$$

The above A represented the optical density of the drug-containing sample. A_b represented the optical density of the cell-free sample, and A_0 represented the optical density of the drug-free sample.

In Vivo Antitumor Efficacy. Subcutaneous xenograft mice models of breast adenocarcinoma were employed to evaluate the therapeutic efficiency of NM/CP6A in vivo, and model mice were affordable and available in our lab. A total of nine six-week-old female BALB/c nude mice were purchased. During the experiment, the animals had good housing and husbandry, and suffering was reduced in accordance with humanitarianism.

A total of 5×10^5 MCF-7 cells in 200 μL of saline were inoculated subcutaneously into the right dorsal flanks of the mice. When the mean tumor volume reached approximately 200 mm^3, the day was set as day 0. Nine BALB/c nude mice were randomly divided into three groups. The PBS group, free NM group (4 mg·kg^{-1}), and NM/CP6A group (4/42 mg·kg^{-1}) were subjected to intravenous (iv) injection in mice at different time points (on days 0, 3, 6, 9, and 12). After the treatment, tumor volumes and weights for each mouse were recorded at different time points. On day 15, the mice were sacrificed by cervical dislocation, and the tumors were separated from the animals and weighed:

$$\text{Volume}\ (\text{mm}^3) = \frac{L \times W^2}{2}$$

The above L represented the largest tumor diameter, and W represented the smallest tumor diameter.

CONCLUSIONS

In conclusion, our study findings have elucidated an available and generalizable approach for supramolecular chemotherapy using host−guest complexation of a cationic chemotherapy medication, NM, by a well-matched macrocycle, CP6A. Complexation by CP6A was found to relieve toxicity of NM in MCF-10A cells. The stronger association of the SPM/CP6A complex helped to replace NM in the macrocyclic cavity. Remarkably, NM/CP6A showed better antitumor potency due to the competitive release of NM by high-concentration SPM. Furthermore, the simultaneous trapping of SPM could exert a synergistic therapeutic effect. The current study proved that direct complexation is a prospective strategy to enhance chemotherapy outcomes, and pillararene derivatives could serve as ideal modules to bring potential benefits for other chemotherapy medications.

ASSOCIATED CONTENT

Supporting Information

The Supporting Information is available free of charge at https://pubs.acs.org/doi/10.1021/acsomega.3c09353.

^{1}H NMR spectra of SPM/CP6A; optimized geometries of the host−guest complex; competitive replacement of NM from the NM/CP6A complex by SPM; in vitro cytotoxicity of CP6A; body weight changes in mice after treatment with CP6A; in vitro cytotoxicity of the host−guest complex; and in vivo antitumor efficacy (PDF)

https://doi.org/10.1021/acsomega.3c09353
ACS Omega 2024, 9, 11829−11835

AUTHOR INFORMATION

Corresponding Author

Jin Long Zhang − *Capital Medical University Affiliated Beijing Tongren Hospital Department of Radiology, Beijing 100730, China;* orcid.org/0000-0003-3158-2130; Email: along0312@126.com

Authors

Xiao Wei Zhang − *Hubei University, Wuhan 430062, China*

Bing Yuan − *Department of Interventional Radiology, Chinese PLA General Hospital, Beijing 100853, China*

Heng Zhang − *Department of Radiology, Chinese PLA General Hospital Second Medical Center, Beijing 100853, China*

Xing Zhi Wang − *Shenyang Pharmaceutical University, Shenyang 117004, China*

Hao Wang − *Shenyang Pharmaceutical University, Shenyang 117004, China*

Hong Wei Zhao − *Capital Medical University Affiliated Beijing Tongren Hospital Department of Radiology, Beijing 100730, China*

Complete contact information is available at: https://pubs.acs.org/10.1021/acsomega.3c09353

Author Contributions

Conception and design, J.L.Z.; analysis and interpretation of the data, H.Z. and B.Y.; performing experiments and drafting of the original paper, X.W.Z., X.Z.W., and H.W.; conception and review, H.W.Z.; final approval of the version to be published, J.L.Z.; all authors agree to be accountable for all aspects of the work.

Notes

The authors declare no competing financial interest.

ACKNOWLEDGMENTS

This research received no external funding.

REFERENCES

(1) Allemani, C.; Matsuda, T.; Di Carlo, V.; et al. Global surveillance of trends in cancer survival 2000−14 (CONCORD-3): analysis of individual records for 37 513 025 patients diagnosed with one of 18 cancers from 322 population-based registries in 71 countries. *Lancet* **2018**, *391*, 1023−1075.

(2) Harbeck, N.; Penault-Llorca, F.; Cortes, J. Breast Cancer. *Nat. Rev. Dis Primers* **2019**, *5*, 66.

(3) Zardavas, D.; Irrthum, A.; Swanton, C.; Piccart, M. Clinical management of breast cancer heterogeneity. *Nat. Rev. Clin Oncol* **2015**, *12*, 381−394.

(4) Britt, K. L.; Cuzick, J.; Phillips, K. A. Key steps for effective breast cancer prevention. *Nat. Rev. Cancer* **2020**, *20*, 417−436.

(5) Eckhardt, B. L.; Francis, P. A.; Parker, B. S.; Anderson, R. L. Strategies for the discovery and development of therapies for metastatic breast cancer. *Nat. Rev. Drug Discov* **2012**, *11*, 479−497.

(6) Love, R. R.; Leventhal, H.; Easterling, D. V.; Nerenz, D. R. Side effects and emotional distress during cancer chemotherapy. *Cancer* **1989**, *63*, 604−612.

(7) Alcindor, T.; Beauger, N. Oxaliplatin: a review in the era of molecularly targeted therapy. *Current oncology (Toronto, Ont.)* **2011**, *18*, 18−25.

(8) Kataoka, K.; Harada, A.; Nagasaki, Y. Block copolymer micelles for drug delivery: design, characterization and biological significance. *Adv. Drug Delivery Rev.* **2001**, *47*, 113−131.

(9) Cabral, H.; Kataoka, K. Progress of drug-loaded polymeric micelles into clinical studies. *J. Controlled Release* **2014**, *190*, 465−476.

(10) Allen, T. M.; Cullis, P. R. Liposomal drug delivery systems: from concept to clinical applications. *Adv. Drug Delivery Rev.* **2013**, *65*, 36−48.

(11) Mu, L. M.; Ju, R. J.; Liu, R.; et al. Dual-functional drug liposomes in treatment of resistant cancers. *Adv. Drug Delivery Rev.* **2017**, *115*, 46−56.

(12) Duan, Q.; Cao, Y.; Li, Y.; et al. pH-responsive supramolecular vesicles based on water-soluble pillar[6]arene and ferrocene derivative for drug delivery. *J. Am. Chem. Soc.* **2013**, *135*, 10542−10549.

(13) Palivan, C. G.; Goers, R.; Najer, A.; Zhang, X.; Car, A.; Meier, W. Bioinspired polymer vesicles and membranes for biological and medical applications. *Chem. Soc. Rev.* **2016**, *45*, 377−411.

(14) Angelos, S.; Khashab, N. M.; Yang, Y. W.; et al. pH clock-operated mechanized nanoparticles. *J. Am. Chem. Soc.* **2009**, *131*, 12912−12914.

(15) Brown, S. D.; Nativo, P.; Smith, J. A.; et al. Gold nanoparticles for the improved anticancer drug delivery of the active component of oxaliplatin. *J. Am. Chem. Soc.* **2010**, *132*, 4678−4684.

(16) Zhou, J.; Yu, G.; Huang, F. Supramolecular chemotherapy based on host-guest molecular recognition: a novel strategy in the battle against cancer with a bright future. *Chem. Soc. Rev.* **2017**, *46*, 7021−7053.

(17) Gao, J.; Li, J.; Geng, W.; et al. Biomarker displacement activation: a general host − guest strategy for targeted phototheranostics in vivo. *J. Am. Chem. Soc.* **2018**, *140*, 4945−4953.

(18) Hu, X.; Gao, J.; Chen, F.; Guo, D. A Host-Guest Drug Delivery Nanosystem for Supramolecular Chemotherapy. *J. Controlled Release* **2020**, *324*, 124−133.

(19) Geng, W.; Sessler, J. L.; Guo, D. Supramolecular prodrugs based on host−guest interactions. *Chem. Soc. Rev.* **2020**, *49*, 2303−2315.

(20) Chen, Y.; Huang, Z.; Xu, J. F.; Sun, Z.; Zhang, X. Cytotoxicity Regulated by Host-Guest Interactions: A Supramolecular Strategy to Realize Controlled Disguise and Exposure. *ACS Appl. Mater. Interfaces* **2016**, *8*, 22780−22784.

(21) Hao, Q.; Chen, Y.; Huang, Z.; Xu, J. F.; Sun, Z.; Zhang, X. Supramolecular Chemotherapy: Carboxylated Pillar[6]arene for Decreasing Cytotoxicity of Oxaliplatin to Normal Cells and Improving Its Anticancer Bioactivity Against Colorectal Cancer. *ACS Appl. Mater. Interfaces* **2018**, *10*, 5365−5372.

(22) Sun, C.; Zhang, H.; Li, S.; et al. Polymeric Nanomedicine with "Lego" Surface Allowing Modular Functionalization and Drug Encapsulation. *ACS Appl. Mater. Interfaces* **2018**, *10*, 25090−25098.

(23) Pegg, A. E.; Casero, R. A., Jr. Current status of the polyamine research field. *Methods in molecular biology (Clifton, N.J.)* **2011**, *720*, 3−35.

(24) Wallace, H. M.; Fraser, A. V.; Hughes, A. A perspective of polyamine metabolism. *Biochem. J.* **2003**, *376*, 1−14.

(25) Thomas, T.; Thomas, T. J. Polyamine metabolism and cancer. *J. Cell. Mol. Med.* **2003**, *7*, 113−126.

(26) Chabner, B. A.; Roberts, T. G., Jr. Timeline: Chemotherapy and the war on cancer. *Nat. Rev. Cancer* **2005**, *5*, 65−72.

(27) Singh, R. K.; Kumar, S.; Prasad, D. N.; Bhardwaj, T. R. Therapeutic journey of nitrogen mustard as alkylating anticancer agents: Historic to future perspectives. *Eur. J. Med. Chem.* **2018**, *151*, 401−433.

(28) Ogoshi, T.; Yamagishi, T. A.; Nakamoto, Y. Pillar-Shaped Macrocyclic Hosts Pillar[n]arenes: New Key Players for Supramolecular Chemistry. *Chem. Rev.* **2016**, *116*, 7937−8002.

(29) Zhang, H.; Liu, Z.; Zhao, Y. Pillararene-based self-assembled amphiphiles. *Chem. Soc. Rev.* **2018**, *47*, 5491−5528.

(30) Chen, J.; Zhang, Y.; Chai, Y.; et al. Synergistic enhancement of the emergency treatment effect of orgaophosphate poisoning by a supramolecular strategy. *Chem. Sci.* **2021**, *12*, 5202−5208.

(31) Jiang, L.; Huang, X.; Chen, D. Supramolecular vesicles coassembled from disulfide-linked benzimidazolium amphiphiles and carboxylated-substitutd pillar[6]arenes that are responsive to five stimuli. *Angew. Chem., Int. Ed.* **2017**, *56*, 2655−2659.

(32) Zhou, J.; Rao, L.; Yu, G.; et al. Supramolecular cancer nanotheranostics. *Chem. Soc. Rev.* **2021**, *50*, 2839−2891.
(33) Hennig, A.; Bakirci, H.; Nau, W. M Label-free continuous enzyme assays with macrocycle-fluorescent dye complexes. *Nat. Methods* **2007**, *4*, 629−632.

https://doi.org/10.1021/acsomega.3c09353
ACS Omega 2024, 9, 11829−11835